Pericoronary fat attenuation index is associated with plaque parameters and stenosis severity in patients with acute coronary syndrome: a cross-sectional study

Runzhi Zhang[1], Zhiguo Ju[2], Yuanyuan Li[1], Yan Gao[1], Hui Gu[1], Ximing Wang[1]

[1]Department of Radiology, Shandong Provincial Hospital Affiliated to Shandong First Medical University, Jinan, China; [2]College of Medical Imaging, Shanghai University of Medicine and Health Science, Shanghai, China

Contributions: (I) Conception and design: All authors; (II) Administrative support: None; (III) Provision of study materials or patients: None; (IV) Collection and assembly of data: R Zhang; (V) Data analysis and interpretation: R Zhang; (VI) Manuscript writing: All authors; (VII) Final approval of manuscript: All authors.

Correspondence to: Ximing Wang. Department of Radiology, Shandong Provincial Hospital Affiliated to Shandong First Medical University, No. 324 Jingwu Road, Jinan, China. Email: wxming369@163.com.

Background: The pericoronary fat attenuation index (FAI) is a novel imaging biomarker of coronary inflammation, which is closely related to development and progression of coronary artery disease (CAD). However, there are limited reports on whether elevated pericoronary FAI values from coronary computed tomography angiography (CCTA) were associated with plaque parameters and coronary stenosis in patients with acute coronary syndrome (ACS). We aimed to assessed that FAI helps to identify high risk of CAD.

Methods: The clinical diagnosis confirmed to the American Heart Association guidelines for ACS. The lesion-specific pericoronary FAI and plague parameters were measured using QAngioCT software. Using a Hounsfield unit (HU) of –70.1 as the threshold value, lesions with a lesion-specific pericoronary FAI value ≥–70.1 HU were allocated to the FAI-positive group and those with a FAI value <–70.1 HU were allocated to the FAI-negative group. The patients were divided into four stenosis groups according to the coronary angiography (CAG) results, and differences in the FAI values among the four groups were analyzed.

Results: A retrospective analysis of 127 ACS patients, including 299 lesions, who underwent CCTA and CAG successively was conducted. The prevalence of vulnerable plaques increased significantly in the FAI-positive group (49.35% *vs.* 23.87%, P<0.001). The area under the curve (AUC) of FAI in the diagnosis of vulnerable plagues was 0.810. Plaques were closer to the coronary ostium [3.32 (2.83, 4.29) *vs.* 4.17 (3.33, 4.95) cm, P<0.001] and more often located in the bifurcated segments of the vessels (50.65% *vs.* 32.43%, P=0.004) in the FAI-positive group than the FAI-negative group. The FAI-positive group also had a higher percentage of diameter stenosis than the FAI-negative group [80.00% (65.00%, 90.00%) *vs.* 60.00% (40.00%, 85.00%), P<0.001]. FAI values were higher in stenoses with a diameter ≥50% than stenoses with a diameter <50%.

Conclusions: The FAI was identified as a novel imaging biomarker of coronary inflammation that is correlated with vulnerable plaque features and stenosis severity.

Keywords: Coronary artery disease (CAD); coronary computed tomography angiography (CCTA); perivascular adipose tissue; vulnerable plagues

Introduction

The World Health Organization recently ranked coronary artery disease (CAD) as the number one leading cause of death worldwide. Patients with acute coronary syndrome (ACS) have a reduced quality of life and a heavy financial burden. The formation of atherosclerotic plaques in the coronary arteries can affect the function of the heart, and ACS are usually associated with vulnerable plaques (1-3).

The relationship between the fat attenuation index (FAI) and CAD has been confirmed in several studies, including the CRISP-CT study (4), which suggested that an elevated pericoronary FAI value indicates a higher risk of cardiac death and a poorer clinical prognosis, and demonstrated that the cut-off of the FAI was –70.1 Hounsfield unit (HU). Based on this threshold, it was further confirmed that the prevalence of vulnerable features is more common in lesions with high pericoronary FAI values in acute non-ST–segment elevation ACS (NSTE-ACS) (5).

Li *et al.* also analyzed the diagnostic value of the FAI for myocardial ischemia by exploring the association between FAI and fractional flow reserve (6). A sub-study on the incidence of coronary syndromes identified by CT illustrated that in addition to the high-risk characteristics of the plaque, plaque location and vessel geometry are also associated with ACS, and plaques with adverse geometric characteristics (i.e., those closer to coronary ostium, and those located at vessel bifurcations and tortuosity) are more likely to develop into vulnerable plaques (7). However, few studies have confirmed the correlation between the FAI and the degree of coronary stenosis.

CCTA is useful for evaluation of plaque feature and coronary stenosis. The vulnerable plaque features, are found to be predictors of major adverse cardiovascular events and plague progression. In addition to plaque features, higher perivascular FAI was revealed to be related to coronary inflammation and high risk of cardiac mortality (3-4,7). Therefore, the present study sought to analyzed the association between the FAI and plague parameters (i.e., vulnerable plaque characteristics, quantitative plaque components, and adverse geometric characteristics) in ACS based on coronary computed tomography angiography (CCTA) and also investigated differences in FAI values among patients with different degrees of coronary stenosis. We aimed to help clinical monitoring the perivascular inflammation and the riskiness of CAD in a non-invasive way. We present the following article in accordance with the STARD reporting checklist (available at https://jtd.amegroups.com/article/view/10.21037/jtd-22-1536/rc).

Methods

Study design and clinical data

The study was conducted in accordance with the Declaration of Helsinki (as revised in 2013). Approval was granted by the Ethics Committee of Shandong Provincial Hospital Affiliated to Shandong First Medical University (SWYX: No. 2022-309). Informed consent was obtained from all individual participants included in the study. We retrospectively collected the data of patients with ACS who underwent CCTA from June 2020 to March 2022 at the Shandong Provincial Hospital Affiliated to Shandong First Medical University. The clinical diagnosis confirmed to the American Heart Association (AHA) guidelines for ACS (myocardial infarction or unstable angina). Patients eligible for enrollment had typical ischemic symptoms and subsequently confirmed by CAG, electrocardiogram (ECG) and cardiovascular biomarkers [cTn (I or T), hs-cTn, etc.]. To be eligible for inclusion in this study, patients had to meet the following inclusion criteria: (I) have complete general clinical data; (II) have complete CCTA data; and (III) have undergone a coronary angiography (CAG) after CCTA. Patients were excluded from the study if they met any of the following exclusion criteria: (I) had a history of myocardial infarction; (II) had undergone coronary artery bypass grafting or stenting; (III) had been treated with triglyceride-lowering drugs (e.g., fibrates and statins); (IV)

Highlight box

Key findings
- Pericoronary FAI may help identify vulnerable plaque features and coronary stenosis in patients with acute coronary syndrome.

What is known and what is new?
- Pericoronary FAI is related to CAD and plaque progression.
- Our study reports an association between the FAI, plaque parameters and stenosis severity in ACS patients. Lesions in the FAI-positive group contained more vulnerable plaques with a higher proportion of necrotic core volume. Lesions with high pericoronary FAI were closer to the coronary ostium and more frequently located in bifurcations. Stenosis severity was positively associated with the pericoronary FAI.

What is the implication, and what should change now?
- Pericoronary FAI may help clinical monitoring the perivascular inflammation and the riskiness of CAD in a non-invasive way.
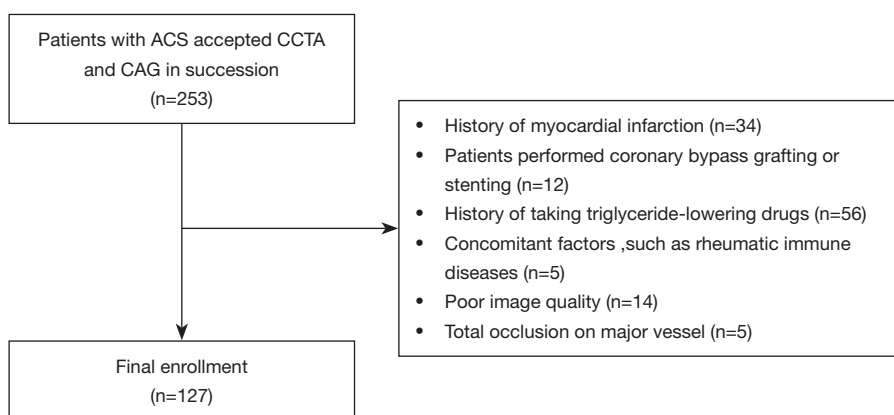
Figure 1 Flow chart of the process for patient inclusion. ACS, acute coronary syndrome; CCTA, coronary computed tomography angiography; CAG, coronary angiography.

had a relevant disease that might also result in increased FAI, such as rheumatic immune diseases; (V) had heavy artifacts and poor-quality CCTA images, or had images of an insufficient quality for the FAI and plague analysis; and/ or (VI) had total occlusion of a major epicardial vessel.

Ultimately, 127 patients (45 female and 82 male), aged 64 years (range, 53–71 years), with a total of 299 lesions, were included in the study (*Figure 1*). The clinical data of the patients (i.e., their gender, age, hypertension, hyperlipidemia, diabetes, history of smoking, and alcohol consumption) and blood biochemical indices were recorded. Hypertension was defined as a systolic blood pressure ≥140 mmHg (1 mmHg =0.133 kPa) or diastolic blood pressure ≥90 mmHg or taking antihypertensive medication. History of smoking was defined as not having quit smoking at the time of CCTA and having quit smoking but for less than 6 months. History of alcohol consumption defined as not abstaining from alcohol at the time of CCTA and having abstained from alcohol for less than 6 months. Diabetes and hyperlipidaemia are the clinical diagnosis (8). The patients were divided into the FAI-positive and FAI-negative groups based on whether their FAI value was ≥−70.1 HU. We measured FAI and plaque parameters of each lesion using post-processing software. Stenosis severity were obtained by the results of CAG.

CCTA protocol

Each CCTA examination was conducted using a 3rd-generation dual-source CT manufactured by Siemens (SOMATOM Force CT, Germany). The procedure for the CCTA examination was as follows: (I) pre-scan preparation: to dilate the coronary arteries and reduce the respiratory motion artifacts, sublingual nitroglycerin spray was used on all patients, except hypotensive patients, and the patients were trained to hold their breath before the examination; (II) contrast injection: the contrast agent (30.0–55.0 mL of non-ionic iohexol) and 0.90% sodium chloride (30.0–55.0 mL) were intravenously injected into the back of the hand of the scanned patient at a 3.5–5.5 mL/s flow rate; (III) scanning: Bolus tracking was used to trigger the acquisition 5 s after an attenuation threshold of 100 Hounsfield units (HU) was reached into the aortic arch. Prospective or retrospective cardiac gating was chosen for use based on the heart rate and respiration of each patient. The scanning parameters were as follows: layer thickness: 0.75 mm; tube voltage: 70–120 kV; and (IV) image post-processing: the best diastolic and systolic phase were automatically reconstructed.

CAG

The Siemens Artis zee floor angiography machine was used to perform the CAG. The conventional angiographic viewing angle for the left coronary artery was as follows: left anterior oblique 60°, left anterior oblique 60° + cranial 25°–35°, left anterior oblique 60° + caudal 25°, right anterior oblique 30°, right anterior oblique 30° + cranial 25°, and right anterior oblique 30° + caudal 25°–35°. The following 3 standard positions were used for the right CAG: standard anterior posterior projection, left anterior oblique 60°, and right anterior oblique 30°, with additional positions as necessary.

Plaque and pericoronary FAI analysis

QAngioCT RE 3.2 (Medis Medical Imaging, Leiden, The Netherlands) software was used to analyze the features of coronary plaque for the main coronary arteries. The software was also used to perform semi-automatic, quantitative assessments of stenosis severity and plaque components. Lesions in all 3 major coronary vessels were assessed. When separate lesions were observed in a major coronary vessel, we evaluated the more severely diseased lesions. For the diffused coronary lesions, the segments were analyzed across the lesion between the proximal normal segment and the distal normal segment. Once a coronary artery was selected for analysis, the vessel and lumen contours were identified, the starting and ending points of the plaque were identified, and software was used to calculate the mean plague burden, maximum plague thickness, and the volume of each component of the plaque of each plaque. For the analysis of the quantitative plaque components, the following HU cut-off values were used for the classification: necrotic core: –30 to 75; fibrofatty plaques: 76–130; fibrous plaques: 131–350; and dense calcified plaques: >351.

Dedicated FAI analysis software (QAngioCT RE 3.2, Medis Medical Imaging, Leiden, The Netherlands) was used for quantification. The pericoronary FAI was interpreted as the mean attenuation on CT for the pericoronary adipose tissue (PCAT) (from –190 to –30 HU) (9). The lesion-based FAI was surveyed around the lesion segments of all 3 major epicardial coronary vessels located within a radial distance from the outer vessel wall equal to the diameter of the respective vessel. Using a novel segmentation algorithm, we only needed to determine the starting and ending points of the plaque to obtain the FAI value. Representative images are presented in *Figure 2*, and demonstrate the mechanism used to measure quantitative plaque components and the perivascular FAI.

To check the consistency of the measurements, a second measurement was performed on a random sample of 20 patients after the completion of the first measurement by two experienced radiologists. The results of two measurements before and after of the same physician were tested for intra-observer reliability, and the measurements taken by two physicians were tested for inter-observer reliability.

Vulnerable plaque features and adverse geometric characteristics

Based on the CT imaging, plaques with 2 or more of the following conditions were considered vulnerable plaques (10,11): (I) positive remodeling: The maximum diameter of the vessel at the location of the plaque >1.1 × [(diameter of the vessel proximal to the plaque + diameter of the vessel distal to the plaque)/2]; (II) spotty calcification: Calcification within the plaque with a diameter of <3 mm; (III) low-attenuation plaque: Plaques with a CT value of <30 HU; (IV) napkin-ring sign: the annular high-density region surrounding a low-density plaque.

Coronary lesions were assessed using the 3 following adverse geometric characteristics (7): (I) the distance from the lesion to the coronary ostium; (II) the location of its formation at vessel bifurcations; and (III) vessel tortuosity, which was defined as the presence of 1 bend >90° or 3 curves of 45° to 90°, by a 3-point angle in the lesion.

The 2 cardiovascular radiologists, who were blinded to the results, analyzed the vulnerable plaque features and adverse geometric characteristics in each lesion.

Statistical analysis

The data analysis was performed using SPSS 26.0 software. The continuous variables with a normal distribution are described as the mean ± standard deviation. The continuous variables with a non-normal distribution are described as the medians and interquartile range and were analyzed using the Mann-Whitney U test. The categorical variables, such as gender and cardiovascular risk factors, are presented as cases and percentages [count (%)] and were analyzed using the chi-squared test. The best diagnostic FAI threshold for the CT vulnerable plaques was evaluated by the receiver operating characteristic (ROC) curve. A Spearman's correlational analysis was used to explore the correlation between FAI and other variables as appropriate. An analysis between groups with different degrees of stenosis was performed by a 1-way analysis of variance test. Intraclass correlations (ICCs) were used to check the consistency of the measurements. A 2-tailed probability (P) value <0.05 was considered statistically significant.

Results

Clinical characteristics

A total of 127 patients (82 male and 45 female), with a total of 299 lesions, and a median age of 64 years (range, 53–71 years), were included in this study. In total, there were 11 cases of acute ST-elevation myocardial infarction, 36 cases of acute non-ST segment elevation myocardial
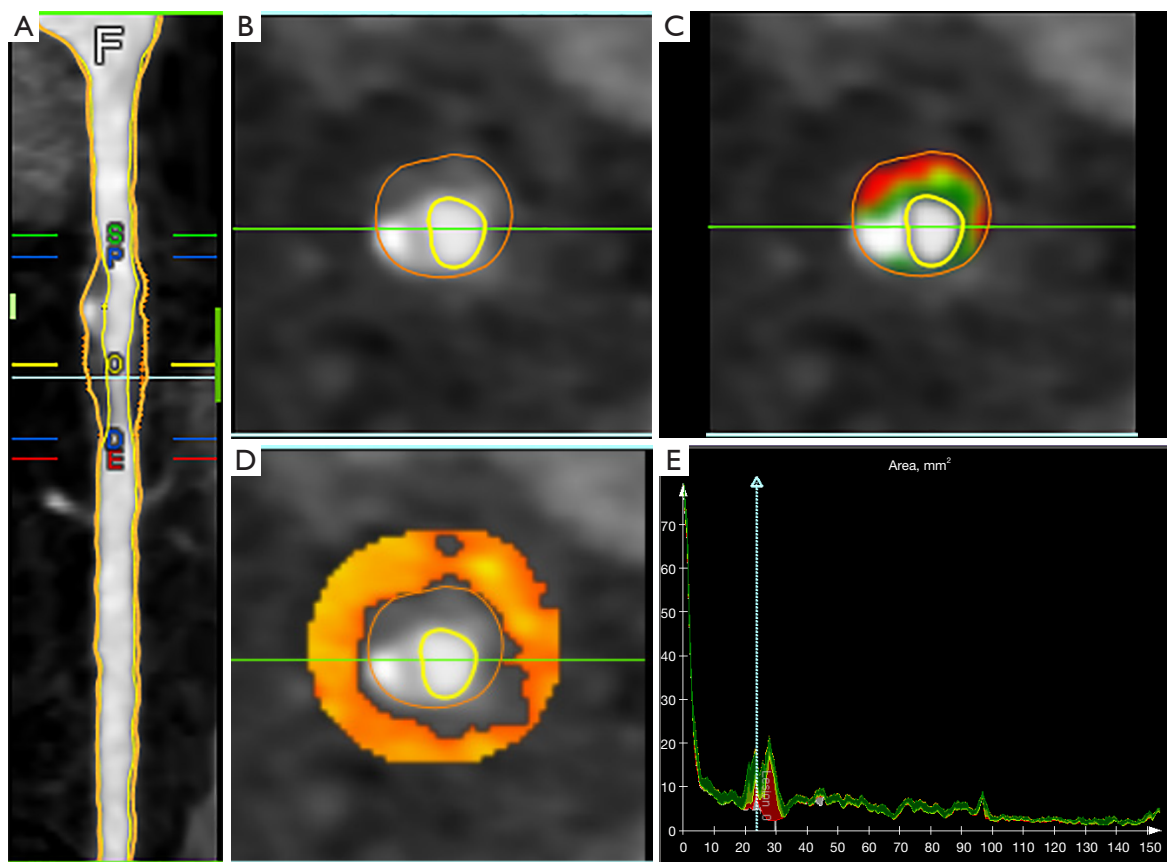
Figure 2 Example of coronary quantitative plaque components and the pericoronary FAI of a RCA lesion. (A) Multiplanar reconstruction of an RCA vessel, where "S" is the starting point and "E" is the ending point of the lesion; (B) transverse section of this lesion; (C) the transverse section is composed of necrotic core tissue (red area), fibrofatty tissue (yellow area), fibrous tissue (green area), and calcification (white area) at the same level of (B); (D) transverse section of the pericoronary FAI at the same level of (B). (E) Line-chart graph of the lumen and vessel area in terms of the distance from the coronary ostium to the lesion. X-axis represents distance from the ostium of the target vessel(mm), y-axis represents lumen and vessel area (mm^2). FAI, fat attenuation index; RCA, right coronary artery.

infarction, and 80 cases of unstable angina. The basic clinical characteristics of the patients are shown in *Table 1*.

Relationship between the pericoronary FAI and plaque parameters and the degree of stenosis

The prevalence of vulnerable plaques was higher in the FAI-positive group than the negative group (49.35% *vs.* 23.87%, P<0.001). In terms of the vulnerable plaque characteristics, low-attenuation plaques (24.68% *vs.* 10.36%, P=0.002) and napkin-ring signs (11.69% *vs.* 4.95%, P=0.042) were more common in the FAI-positive group than the FAI-negative group; No notable difference was observed in the rate of spotty calcification or positive remodeling between the two groups. The FAI values were higher in the vulnerable

plaques than the non-vulnerable plaques [–71.00 (–73.00, –65.00) *vs.* –80.00 (–86.00, –75.00) HU, P<0.001]. The ROC curve showed that the best threshold for the FAI to diagnose vulnerable plaques was –75.5 HU. The area under the curve (AUC) was 0.810 [95% confidence interval (CI): 0.761–0.853, P<0.001], the sensitivity was 87.91%, and the specificity was 74.52% (*Figure 3*).

In relation to the quantitative plaque components, the mean plaque burden [48.07% (40.20%, 55.82%) *vs.* 40.55% (30.01%, 53.63%), P=0.001] was higher, and the maximum plaque thickness [1.93 (1.46, 2.67) *vs.* 1.77 (1.25, 2.29) mm, P=0.026] was thicker in the FAI-positive group than the FAI-negative group. In relation to the examination of the quantitative plague features, the necrotic core volume percentage [23.05% (15.31%, 32.88%) *vs.* 15.23% (9.51%,

4870

Zhang et al. FAI and plaque parameters in ACS

Table 1 Basic clinical characteristics

Characteristics	Value
Age, years	64 [53, 71]
Sex, male/female	82/45
Hypertension, n (%)	83 (65.35)
Diabetes mellitus, n (%)	47 (37.01)
Hyperlipidemia, n (%)	16 (12.60)
History of smoking, n (%)	45 (35.43)
History of alcohol consumption, n (%)	39 (30.71)
Biochemical assessment	
CPR, mg/L	2.11 [0.91, 3.24]
ALT, U/L	21.00 [15.00, 29.00]
Creatinine, μmol/L	70.37 [59.35, 80.76]

Data are presented as n, n (%) or median [lower, upper quartile].
CRP, C-reaction protein; ALT, alanine aminotransferase.

AUC =0.810
P<0.001
Cutoff =−75.5HU
Sensitivity =87.91%
Specificity =74.52%
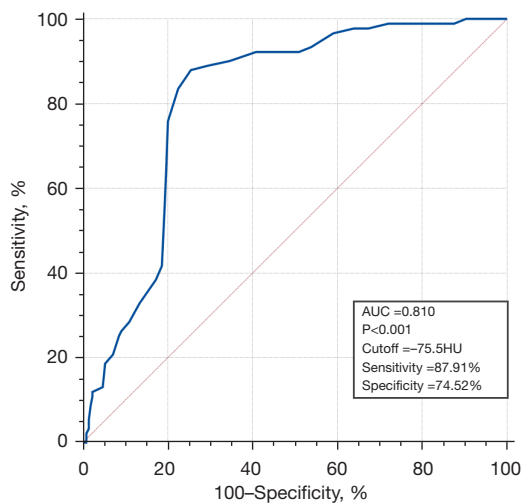
Figure 3 ROC curve for the vulnerable plaques diagnosed by the FAI. ROC, receiver operating characteristic; FAI, fat attenuation index; AUC, area under the curve.

23.03%), P<0.001] was higher, and the fibrous volume [34.82% (23.02%, 51.22%) *vs.* 40.82% (29.61%, 53.64%), P=0.038] was lower in the FAI-positive group than the FAI-negative group. Necrotic core volume [25.19 (10.22, 50.85) *vs.* 15.13 (6.30, 32.23) mm^3, P=0.001] was higher in the FAI-positive group than the FAI-negative group. However, no statistical differences were observed between the 2 groups in terms of the remaining absolute volume of the plaque

components, percentage of fibrofatty volume, and dense calcified volume.

Among the adverse geometric characteristics of the vessels, the plaques were closer to the coronary ostium [3.32 (2.83, 4.29) *vs.* 4.17 (3.33, 4.95) cm, P<0.001], and more often located in the bifurcated segments of the vessels (50.65% *vs.* 32.43%, P=0.004) in the FAI-positive group than the FAI-negative group. No significant difference was observed in the rates of tortuous segments of the vessels between the 2 groups. The degree of coronary artery stenosis was higher in the FAI-positive group than the negative group [80.00% (65.00%, 90.00%) *vs.* 60.00% (40.00%, 85.00%), P<0.001] (*Table 2*).

We also performed a correlation analysis and found that the following indicators were positively correlated with the FAI: the mean plague burden (Spearman's correlation coefficient r=0.325, P<0.001), the necrotic core volume (r=0.354, P<0.001), and the necrotic core volume percentage (r=0.501, P<0.001). However, the distance from the coronary ostium to the lesion (r=−0.407, P<0.001) was negatively correlated with the FAI (*Figure 4*).

We further analyzed the degree of stenosis based on the CAG results showing the degree of stenosis. We divided the patients into four groups based on the following stenosis diameters: 0–24%, 25–49%, 50–69%, and ≥70%. The analysis of the differences in the FAI between the groups showed that the degree of stenosis did not differ significantly between the two groups at <50%, but the degree of stenosis did differ significantly in the remaining pairwise comparisons (*Figure 5*, *Table 3*).

We also examined the intra-/inter-observer reliability of the quantitative plague features. As *Table 4* shows, there was good consistency among the measurements.

Discussion

A number of conclusions can be drawn from our study. First, the FAI-positive group had a higher proportion of vulnerable plaques, napkin-ring signs, and low-attenuation plagues than the FAI-negative group, and the FAI values were higher in the vulnerable plaques than the non-vulnerable plaques. Second, the examination of the quantitative plaque components showed that the FAI-positive group had a larger necrotic core volume and lower fibrous volume than the FAI-negative group. Third, the analysis of the adverse geometric characteristics of the vessels showed that the plaques in the FAI-positive group were closer to the coronary ostium and more frequently

Table 2 Plaque parameters and stenosis ratios with high or low pericoronary FAI values

Variables	FAI ≥−70.1 (n=77)	FAI <−70.1 (n=222)	P value
CT vulnerable plaque features, n (%)			
Vulnerable plaque	38 (49.35)	53 (23.87)	<0.001
Positive remodeling	30 (38.96)	66 (29.73)	0.135
Spotty calcification	35 (45.45)	77 (34.68)	0.092
Low-attenuation plaque	19 (24.68)	23 (10.36)	0.002
Napkin-ring sign	9 (11.69)	11 (4.95)	0.042
Quantitative plaque features			
Plaque volume, mm^3	147.13 (68.45, 202.50)	100.78 (53.07, 190.17)	0.090
Mean plaque burden, %	48.07 (40.20, 55.82)	40.55 (30.01, 53.63)	0.001
Maximal plaque thickness, mm	1.93 (1.46, 2.67)	1.77 (1.25, 2.29)	0.026
Absolute volume of plaque components			
Fibrous volume, mm^3	46.31 (22.41, 81.27)	39.45 (21.13, 72.66)	0.446
Fibrofatty volume, mm^3	25.32 (8.71, 44.29)	17.11 (7.26, 37.01)	0.063
Necrotic core volume, mm^3	25.19 (10.22, 50.85)	15.13 (6.30, 32.23)	0.001
Dense calcified volume, mm^3	11.38 (3.78, 37.47)	10.03 (1.96, 40.63)	0.434
Percentage of plaque components			
Fibrous volume, %	34.82 (23.02, 51.22)	40.82 (29.61, 53.64)	0.038
Fibrofatty volume, %	18.20 (10.21, 28.43)	16.49 (8.28, 29.99)	0.541
Necrotic core volume, %	23.05 (15.31, 32.88)	15.23 (9.51, 23.03)	<0.001
Dense calcified volume, %	9.67 (4.00, 29.79)	12.09 (3.52, 32.61)	0.756
Adverse geometric characteristics			
Distance from the coronary ostium to lesion, cm	3.32 (2.83, 4.29)	4.17 (3.33, 4.95)	<0.001
Bifurcations, n (%)	39 (50.65)	72 (32.43)	0.004
Vessel tortuosity, n (%)	2 (2.60)	3 (1.35)	0.827
Stenosis ratio, %	80.00 (65.00, 90.00)	60.00 (40.00, 85.00)	<0.001

Data are presented as n (%) or median (lower, upper quartile). FAI, fat attenuation index; HU, Hounsfield unit; CT, computed tomography.

located in bifurcations. Fourth, the FAI-positive group had more severe stenosis, and the FAI values for stenosis with a diameter ≥50% were significantly higher than those for stenosis with a diameter <50%, and in vessels with stenosis of ≥50%, the more severe the stenosis, the higher the FAI values, indicating that the FAI tended to increase as stenosis increased. Together, these results indicate that the FAI can be used as a novel biomarker of pericoronary inflammation, and that the FAI is correlated with the vulnerable plaque characteristics and adverse geometric characteristics of the vessel, and the degree of stenosis.

Previous research has shown that adipose tissue may be involved in the regulation of cardiac metabolism (12). Further, coronary arteries and PCAT interact via paracrine secretions (13). Under normal conditions, PCAT secretes factors that protect blood vessels (14,15), including via the promotion of vasodilation, and anti-inflammatory and antioxidant properties. Once coronary plaques are formed, this balance is disturbed and factors secreted by the vessel wall affect the differentiation of PCAT, changing the phenotype of PCAT from a protective type to an inflammatory type, and the resulting inflammatory
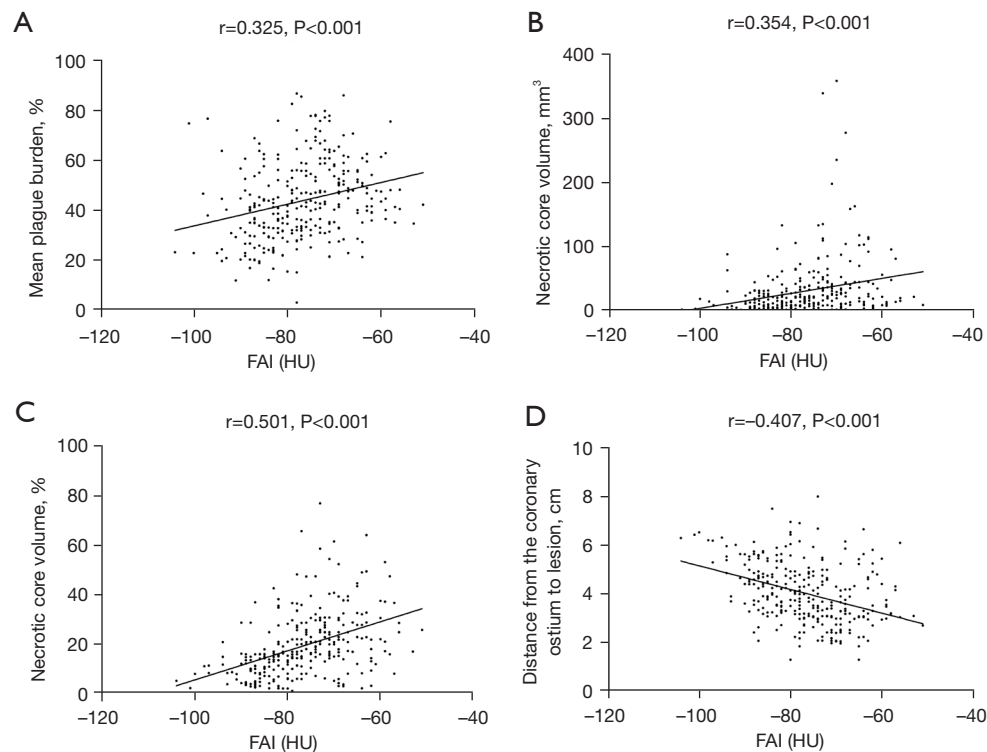
4872

Zhang et al. FAI and plaque parameters in ACS

Figure 4 Correlation between the FAI and the mean plague burden (A), necrotic core volume (B), necrotic core volume percentage (C), and distance from the coronary ostium to the lesion (D). FAI, fat attenuation index; HU, Hounsfield unit.
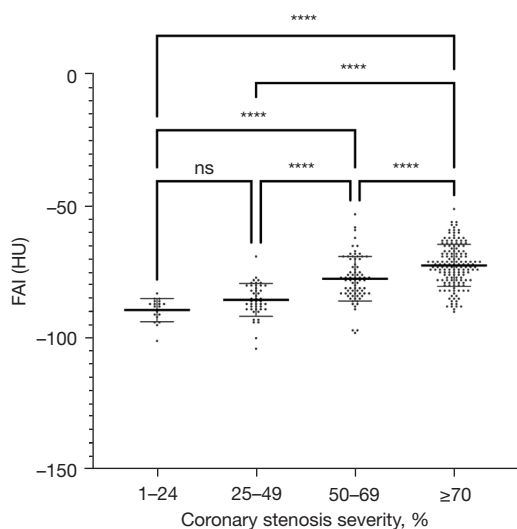

Figure 5 FAI values corresponding to the different stenosis groups. ns, no significant difference (P=0.067); ****, P<0.001. FAI, fat attenuation index; HU, Hounsfield unit.

Table 3 The FAI values between groups with different degrees of stenosis

Stenosis ratio, %	n	FAI (HU)
1–24	19	−89.32±4.41
25–49	46	−85.46±6.24
50–69	77	−77.47±8.45
≥70	157	−72.38±7.99

FAI, fat attenuation index; HU, Hounsfield unit.

reaction of PCAT causes changes in the aqueous phase (16). Similarly, changes in PCAT also affect the vessel wall, accelerating the progression of coronary plaques and aggravating their instability (9). Kohchi *et al.* (17) dissected tissue surrounding the extravasation at the plaque that died as a result of an adverse cardiovascular event, and found that PCAT contains numerous inflammatory cells and

Table 4 ICCs were used to check the consistency of the measurements

Variables	Intra-observer reliability ICC	Inter-observer reliability ICC
FAI	0.980	0.977
Plague volume	0.985	0.972
Mean plaque burden	0.977	0.952
Maximal plaque thickness	0.952	0.918
Fibrous volume	0.978	0.957
Fibrofatty volume	0.894	0.856
Necrotic core volume	0.958	0.913
Dense calcified volume	0.974	0.961
Fibrous volume	0.976	0.964
Fibrofatty volume	0.966	0.956
Necrotic core volume	0.971	0.950
Dense calcified volume	0.943	0.905
Distance from the coronary ostium	0.962	0.947

ICC, intraclass correlations; FAI, fat attenuation index.

also pathologically confirmed the involvement of adipose tissue inflammatory infiltration around the plaque in plaque formation and progression.

Intravascular ultrasound (IVUS) and optical coherence tomography (OCT) are the gold standards for confirming vascular inflammation; however, neither technique can visualize the whole coronary tree, and as both techniques are invasive and costly, they are difficult to use clinically (18,19). CCTA is currently used in coronary artery disease as a 1st-line test and has high diagnostic and prognostic value (20-22). PCAT is a newly identified type of adipose tissue that is distinct from normal subcutaneous and visceral adipose tissue and can be used as an independent indicator of pericoronary inflammation (23). The FAI measures the CT attenuation gradient in a non-invasive manner by monitoring the composition of PCAT and its spatial displacement, which can easily be obtained around any segment of the coronary artery.

Goeller confirmed that the FAI proximal to the plaque indicates perivascular inflammation, enabling the early identification of vulnerable plaques (24). A subsequent study (5) also analyzed the association between the pericoronary FAI and characteristics of vulnerable plaques in low-risk ACS (NSTE-ACS). Referring to the cut-off value settings of previous studies (4-6), our study further analyzed the association between the FAI and the vulnerable plaque characteristics in each type of ACS. We found that

the FAI-positive group contained more vulnerable plaques and a higher proportion of low-attenuation plaques than the FAI-negative group, which corresponds to the results of previous studies (5,25). The present study also found a higher proportion of napkin-ring signs in the FAI-positive group than the FAI-negative group. However, a study by Sun (5) concluded that there was no difference in napkin-ring signs but that there was a difference in spotty calcification between the two groups. Our findings also confirmed that the napkin-ring sign and low-attenuation plaque can be used as CCTA imaging substitutes for large necrotic cores in thin-cap fibroatheromas (26-29).

The quantitative plaque parameters measured using QAngioCT software showed that the plaque burden, maximum plaque thickness, and the necrotic core volume percentage were higher in the FAI-positive group than the FAI-negative group, which is also consistent with the outcomes reported in IVUS (30). These results also confirm that unstable plaques are characterized by a large necrotic core and thin-cap fibroatheromas.

The present study concluded that plaques in the FAI-positive group were more frequently located in proximal, bifurcated segments, which suggests that the geometry of the vessel in which the plaque is located and the distance from the proximal segment of the coronary artery also affect pericoronary inflammation. Our study concluded that

4874

Zhang et al. FAI and plaque parameters in ACS

the FAI values were higher in the vulnerable plaques than the non-vulnerable plaques, and the best threshold for the FAI to diagnose vulnerable plaques was –75.5 HU; thus, patients with a FAI value >–75.5 HU are more likely to have vulnerable plaques. The FAI has good diagnostic efficacy for vulnerable plaques (AUC =0.810). All the above findings indicate that the FAI and plaque interactions are involved in the progression of coronary atherosclerosis.

In addition to the results of Sun *et al.* (5), which was limited to NSTE-ACS, we examined lesions with stenosis of <50% and included 3 types of ACS. Furthermore, we investigated the correlation between stenosis and the FAI. We classified the coronary arteries into 4 different levels of stenosis based on results obtained using the gold-standard CAG. Our results showed that the narrower the coronary artery, the higher the FAI value and the more severe the degree of pericoronary inflammation.

Our study confirmed and extended the results of previous studies (5-7). To the best of our knowledge, our study is the first study to report a significant correlation between the FAI, adverse geometric characteristics and stenosis severity in ACS lesions. Notably, we confirmed that vulnerable plaque features are associated with increased FAI values and that there is a correlation between AGCs and FAI. Finally, we further explored differences in FAI values across various degrees of stenosis, and observed that the FAI values tended to increase as the degree of stenosis increased.

This study had several limitations. First, it was a single-center research study. Second, no follow-up observations were available to compare before and after plaque progression in the FAI-positive group. Thus, we will conduct a prospective study using a larger sample size to further validate the results of this study. Third, under the guidelines (31), patients who have undergone CCTA before CAG in ACS have a low-to-intermediate risk level. Thus, patients with severe inflammation who required urgent and invasive treatment may have been excluded from the present study.

Conclusions

As a novel inflammatory biomarker, the FAI can identify vulnerable plaque features and is correlated with adverse geometric characteristics and coronary stenosis. The FAI values for stenosis with a diameter ≥50% were significantly higher than those for stenosis with a diameter <50%, indicating that the FAI tended to increase as the severity of the stenosis increased. FAI may help monitoring the perivascular inflammation and the riskiness of CAD.

References

1. Min JK, Shaw LJ, Devereux RB, et al. Prognostic value of multidetector coronary computed tomographic angiography for prediction of all-cause mortality. J Am

Coll Cardiol 2007;50:1161-70.

2. Yu M, Li W, Lu Z, et al. Quantitative baseline CT plaque characterization of unrevascularized non-culprit intermediate coronary stenosis predicts lesion volume progression and long-term prognosis: A serial CT follow-up study. Int J Cardiol 2018;264:181-6.

3. Yu M, Lu Z, Li W, et al. Coronary plaque characteristics on baseline CT predict the need for late revascularization in symptomatic patients after percutaneous intervention. Eur Radiol 2018;28:3441-53.

4. Oikonomou EK, Marwan M, Desai MY, et al. Non-invasive detection of coronary inflammation using computed tomography and prediction of residual cardiovascular risk (the CRISP CT study): a post-hoc analysis of prospective outcome data. Lancet 2018;392:929-39.

5. Sun JT, Sheng XC, Feng Q, et al. Pericoronary Fat Attenuation Index Is Associated With Vulnerable Plaque Components and Local Immune-Inflammatory Activation in Patients With Non-ST Elevation Acute Coronary Syndrome. J Am Heart Assoc 2022;11:e022879.

6. Li JH, Tang CX, Liu TY, et al. Association of coronary perivascular fat attenuation index, the parameters of plaque and fractional flow reserve. Zhonghua Yi Xue Za Zhi 2021;101:3214-20.

7. Han D, Lin A, Kuronuma K, et al. Association of Plaque Location and Vessel Geometry Determined by Coronary Computed Tomographic Angiography With Future Acute Coronary Syndrome-Causing Culprit Lesions. JAMA Cardiol 2022;7:309-19.

8. Wang Q, Zhao Y, Wang X, et al. Association between asymptomatic intracranial arterial stenosis and insulin resistance or diabetes mellitus: a cross-sectional study in rural Shandong, China. BMJ Open Diabetes Res Care 2020;8:e001788.

9. Antonopoulos AS, Sanna F, Sabharwal N, et al. Detecting human coronary inflammation by imaging perivascular fat. Sci Transl Med 2017;9:eaal2658.

10. Achenbach S. Imaging the Vulnerable Plaque on Coronary CTA. JACC Cardiovasc Imaging 2020;13:1418-21.

11. Small GR, Chow BJW. CT Imaging of the Vulnerable Plaque. Curr Treat Options Cardiovasc Med 2017;19:92.

12. Badimon L, Cubedo J. Adipose tissue depots and inflammation: effects on plasticity and resident mesenchymal stem cell function. Cardiovasc Res 2017;113:1064-73.

13. Margaritis M, Antonopoulos AS, Digby J, et al. Interactions between vascular wall and perivascular adipose tissue reveal novel roles for adiponectin in the regulation of endothelial nitric oxide synthase function in human vessels. Circulation 2013;127:2209-21.

14. Akoumianakis I, Antoniades C. The interplay between adipose tissue and the cardiovascular system: is fat always bad? Cardiovasc Res 2017;113:999-1008.

15. Antonopoulos AS, Margaritis M, Coutinho P, et al. Adiponectin as a link between type 2 diabetes and vascular NADPH oxidase activity in the human arterial wall: the regulatory role of perivascular adipose tissue. Diabetes 2015;64:2207-19.

16. Elnabawi YA, Oikonomou EK, Dey AK, et al. Association of Biologic Therapy With Coronary Inflammation in Patients With Psoriasis as Assessed by Perivascular Fat Attenuation Index. JAMA Cardiol 2019;4:885-91.

17. Kohchi K, Takebayashi S, Hiroki T, et al. Significance of adventitial inflammation of the coronary artery in patients with unstable angina: results at autopsy. Circulation 1985;71:709-16.

18. Mushenkova NV, Summerhill VI, Zhang D, et al. Current Advances in the Diagnostic Imaging of Atherosclerosis: Insights into the Pathophysiology of Vulnerable Plaque. Int J Mol Sci 2020;21:2992.

19. Stone GW, Maehara A, Lansky AJ, et al. A prospective natural-history study of coronary atherosclerosis. N Engl J Med 2011;364:226-35.

20. Task Force Members; Montalescot G, Sechtem U, et al. 2013 ESC guidelines on the management of stable coronary artery disease: the Task Force on the management of stable coronary artery disease of the European Society of Cardiology. Eur Heart J 2013;34:2949-3003.

21. Chen YD, Fang WY, Chen JY, et al. Chinese expert consensus on the non-invasive imaging examination pathways of stable coronary artery disease. J Geriatr Cardiol 2018;15:30-40.

22. Schmermund A, Eckert J, Schmidt M, et al. Coronary computed tomography angiography: a method coming of age. Clin Res Cardiol 2018;107:40-8.

23. Gealekman O, Gurav K, Chouinard M, et al. Control of adipose tissue expandability in response to high fat diet by the insulin-like growth factor-binding protein-4. J Biol Chem 2014;289:18327-38.

24. Goeller M, Achenbach S, Cadet S, et al. Pericoronary Adipose Tissue Computed Tomography Attenuation and High-Risk Plaque Characteristics in Acute Coronary Syndrome Compared With Stable Coronary Artery Disease. JAMA Cardiol 2018;3:858-63.

25. Dai X, Deng J, Yu M, et al. Perivascular fat attenuation

index and high-risk plaque features evaluated by coronary CT angiography: relationship with serum inflammatory marker level. Int J Cardiovasc Imaging 2020;36:723-30.

26. Seifarth H, Schlett CL, Nakano M, et al. Histopathological correlates of the napkin-ring sign plaque in coronary CT angiography. Atherosclerosis 2012;224:90-6.

27. Motoyama S, Kondo T, Anno H, et al. Atherosclerotic plaque characterization by 0.5-mm-slice multislice computed tomographic imaging. Circ J 2007;71:363-6.

28. Crea F, Libby P. Acute Coronary Syndromes: The Way Forward From Mechanisms to Precision Treatment. Circulation 2017;136:1155-66.

29. Mangge H, Almer G. Immune-Mediated Inflammation in Vulnerable Atheroscle-rotic Plaques. Molecules 2019;24:3072.

30. Pu J, Mintz GS, Brilakis ES, et al. In vivo characterization of coronary plaques: novel findings from comparing greyscale and virtual histology intravascular ultrasound and near-infrared spectroscopy. Eur Heart J 2012;33:372-83.

31. Collet JP, Thiele H, Barbato E, et al. 2020 ESC Guidelines for the management of acute coronary syndromes in patients presenting without persistent ST-segment elevation: The Task Force for the management of acute coronary syndromes in patients presenting without persistent ST-segment elevation of the European Society of Cardiology (ESC). Eur Heart J 2022;42:1289-367.